

## Polypropylene–rubber blends: 3. The effect of the test speed on the fracture behaviour

A. van der Wal<sup>1</sup>, R.J. Gaymans\*

*Laboratory of Polymer Technology, Department of Chemical Technology, Twente University, P.O. Box 217, NL-7500 AE, Enschede, The Netherlands*

Received 10 March 1997; received in revised form 13 January 1998; accepted 6 May 1998

---

### Abstract

Polypropylene–EPDM blends were prepared on a twin screw extruder with a rubber content 0–40 vol%. On these materials the yield strength and the notched tensile behaviour was studied as function of test speed ( $10^{-4}$ –10 m/s). With an infrared temperature camera the heat development in the notched samples is studied as function of test speed. On fractured materials the structure of the deformation zone is studied in the middle of the sample, perpendicular to the fracture plane. The yield strength increases with the strain rate and at high rates this increase is stronger. The fracture energy shows a complex relationship with test speed. At low test speeds the fracture energy decreases rapidly with test speed. At intermediate test speeds however the fracture energy increases with increasing test speed. On the micrographs of the high speed deformed samples the formation of a melt zone was observed. The temperature rise in the notched samples starts at approximately  $10^{-5}$  m/s, and increases almost linearly with the logarithm of the test speed. At 10 m/s a surface temperature increase to 90°C was observed. © 1999 Elsevier Science Ltd. All rights reserved.

**Keywords:** Polypropylene–rubber; Rubber content; Strain rate effects

---

### 1. Introduction

Polypropylene (PP) is a semi-crystalline polymer with very interesting mechanical and thermal properties. For application as engineering plastic however its toughness and, in particular, its notched toughness is not sufficient. PP shows under impact conditions a clear brittle–ductile transition with increasing temperature.

The impact strength of polypropylene can be considerably improved by blending in a rubber. In this way super ductile materials are obtained. The fracture behaviour of rubber toughened polypropylene strongly depends on the blend morphology [1,2] and the test conditions such as temperature and test speed [1]. The PP–rubber blends are ductile to very low temperatures and considerable plastic deformation is taking place in the notch and during crack propagation.

By contrast to the effect of the test temperature little attention has been paid to the influence of the test speed. The effect of test speed is rather complicated since for the strongly plastically deforming materials the deformation energy is to a large extent dissipated as heat [3]. With

increasing test speed the deformation process changes from isothermal to adiabatic [3,4]. Consequently, the temperature rise at the crack tip during crack propagation increases with increasing test speed [4]. The effect of the test speed has been studied on rubber toughened nylon-6 [5–7]. These ductile blends were found to have at high test speed an increase in fracture energy with increasing test speed. This unusual behaviour was explained by a thermal blunting mechanism. The strong plastic deformation at the crack tip resulted in the formation of a relaxation zone in front of the crack tip [5,7]. This relaxation zone just beneath the fracture surface has a thickness of 5  $\mu\text{m}$ . In SAN–PB a very thin relaxation layer (0.5  $\mu\text{m}$ ) was also observed [8].

The fracture toughness ( $K_{Ic}$ ), measured under plain strain conditions, of polymers has been studied as function of test speed [9–12]. The  $K_{Ic}$  values were found to depend on sample thickness and test speed. At high test speeds during crack propagation (under brittle conditions) a molecular thin melt layer (thermal decohesion zone) is formed [11]. For ductile materials like rubber modified PP the  $K_{Ic}$  was found to increase with test speed [13]. This increase was attributed to thermal blunting of the crack tip. They assumed that crack tip blunting is due to thermal softening of the plastic deformation zone [13] (not melting) and possibly also due to dynamic effects [14].

PP–rubber blends are mainly applied in temperature and

---

\* Corresponding author.

<sup>1</sup> Present address: Resina Chemie, 9607 PS Foxhol, The Netherlands.

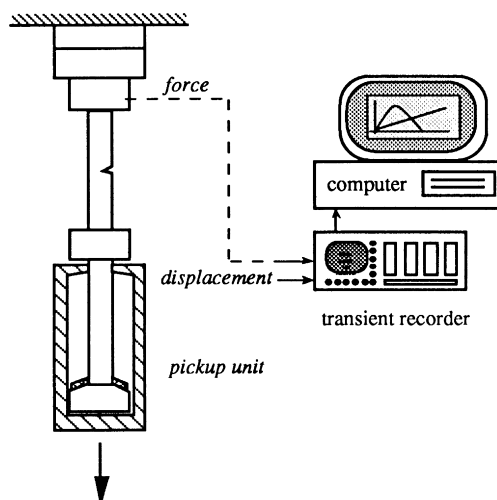


Fig. 1. Test setup high speed tensile tester.

test speed region where it behaves ductile. For this material the brittle–ductile transition is important. The brittle–ductile transition temperature of PP–EPDM blends at high and low speeds has been studied as function of rubber content [1] and particle size [2]. The transition at the high speed was sharp (discontinuous) while at the low speed (1 mm/s) it was gradual.

In the present paper the effect of the test speed on the deformation and fracture behaviour of PP–EPDM blends is studied at 20°C from  $10^{-5}$ –10 m/s.

## 2. Experimental

### 2.1. Specimen preparation

The materials used constitute a polypropylene homopolymer (Vestolen P7000, Vestolen GmbH) with an MFI of 2.4 (230°C, 21.6 N) and an EPDM rubber (Keltan 820, DSM). A series of blends with varying rubber content was prepared by diluting a PP–EPDM (60/40 vol%) extrusion master blend. Rectangular bars and dumb-bell-shaped specimens were prepared by injection moulding. The blending

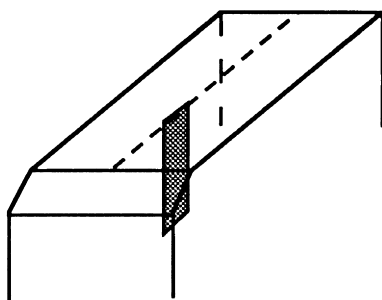


Fig. 2. Sample position for SEM fractography. The micrographs refer to the shaded area.

Table 1

Technical data for a IR temperature camera equipped with a close-up lens (Data from data sheet [13])

Detector	HgCdTe
Spectral range	8–12 $\mu\text{m}$
Temperature range	–20–1500°C
Temperature resolution	0.06°C
Spatial resolution	0.13 mm spot size
Time resolution	140 $\mu\text{s}$

and injection moulding processes are described in detail elsewhere [1].

### 2.2. Tensile test

The tensile tests were carried out on the dumb-bell-shaped specimen (ISO R527-1,  $10 \times 3 \times 115$  mm) on a Schenck servo-hydraulic tensile machine (Fig. 1). This apparatus is especially designed for high speed testing. The studied clamp speeds range is from  $10^{-5}$  to 10 m/s. At high test speeds a pick-up unit is used to allow the piston to reach the desired test speed before loading the specimen. All moving parts are made of titanium in order to diminish inertial effects. The contact between the pick-up unit and the lower clamp is damped by a rubber damping pad. The force is measured using a piezo-electric force transducer located between the upper clamp and the cross head. Force and piston displacement are recorded using a transient recorder (sample rate 2 MHz). After completion of the test, the results are processed by a computer.

### 2.3. SEN tensile test

The fracture behaviour was studied by a tensile test on the notched bars referred to as a single-edge notch (SEN) tensile test. The injection moulded bars (ISO 180/1,  $74 \times 10 \times 4$  mm) had a single-edge 45°V-shaped notch (depth 2 mm, tip radius 0.25 mm), milled in the specimens. The test (five measurements) was carried out on the Schenck servo-hydraulic tensile machine.

### 2.4. SEM fractography

The deformation mechanism was studied by post-mortem SEM analysis of the fracture zone. The sample position is shown in Fig. 2. The area of interest (shaded area in Fig. 2) is perpendicular to the fracture surface, and parallel to the crack growth direction. Samples were taken from the specimens with a fresh razor blade. The samples were smoothed down on a polishing machine to avoid deformation during the trimming procedure. The finishing preparation was carried out by cryotomography at –100°C with a diamond knife. The final surface was sputter-coated with a gold layer and investigated with a Hitachi S-800 field emission SEM.

Table 2  
Initial deformation rates

Cross head speed (m/s)	Tensile (100 mm) deformation rate (s <sup>-1</sup> )	SEN (45 mm) deformation rate (s <sup>-1</sup> )
10 <sup>-5</sup>	10 <sup>-3</sup>	2.78 × 10 <sup>-3</sup>
10 <sup>-4</sup>	10 <sup>-2</sup>	2.78 × 10 <sup>-2</sup>
10 <sup>-3</sup>	10 <sup>-1</sup>	2.78 × 10 <sup>-1</sup>
10 <sup>-2</sup>	1	2.78
10 <sup>-1</sup>	10	2.78 × 10 <sup>1</sup>
1	10 <sup>2</sup>	2.78 × 10 <sup>2</sup>
10	10 <sup>3</sup>	2.78 × 10 <sup>3</sup>

### 2.5. Infrared thermography

The temperature rise during fracture was measured with an infrared camera (IQ 812 system from Flir Systems). Technical data for the camera used are listed in Table 1 [15]. The video signal of the IR camera was recorded by a computer.

## 3. Results and discussion

The influence of test speed on the mechanical properties of PP–EPDM blends was studied with a tensile and a single edged notched tensile test at room temperature. The rubber content of the blends was varied. The influence of test temperature on these blends at 1 mm/s and 1 m/s have also been studied [1]. The influence of test speed is studied by varying the clamp speed from 10<sup>-5</sup> to 10 m/s. PP and some PP–EPDM materials deform with necking. The deformation rate can be calculated for the part where the deformation proceeds homogeneously, i.e. tensile test before the yield point. For the notched samples, the material between the clamps is elastic deformed, but the elastic deformation ahead of the notch is 20% higher as the sample there is 20% smaller. The strain rates are calculated for the tensile samples (100 mm effective length) and for the notched tensile samples (effective sample length of 45 mm) (Table 2). Beyond the yield point the deformation is inhomogeneous and this is particularly the case in presence of a notch. For this region strain rates are difficult to obtain.

The particle size data of the studied blends are shown in

Table 3  
Particle sizes for the PP–EPDM blends [1]

Rubber content [vol%]	$D_n^a$ [μm]	$D_w^b$ [μm]
5	0.25	0.50
10	0.28	0.67
20	0.34	0.69
30	0.42	0.86
40	0.67	0.92

<sup>a</sup>  $D_n$  = number average particle size ( $\sum n_i d_i / \sum n_i$ ).

<sup>b</sup>  $D_w$  = weighted average particle size ( $\sum n_i d_i^2 / \sum n_i d_i$ ).

Table 3. The particle size increases with increasing rubber content. This particle size difference was found to have only a small effect [1]. The tensile properties and the physical properties of the blends are reported elsewhere [1].

### 3.1. Tensile test

In a tensile test PP and PP–EPDM blends deform with necking and have high fracture strains. The yield stress of polypropylene and the 15 and 30 vol% blend is studied as function of test speed (Fig. 3). The yield stress increases almost linearly with the logarithm of the test speed (strain rate) with a deviation at higher test speeds. The yield strength of the blends are lower [1]. Over the whole studied strain rate range the yield strength of the blends are similar to PP.

### 3.2. SEN tensile test

The fracture behaviour was studied as a function of test speed by a SEN tensile test. The fracture process may be divided in two stages: the initiation and the crack propagation stage (Fig. 4). During initiation the stress builds up at the notch tip, but is too low to enable crack propagation. Crack propagation begins at or past the stress maximum in the stress displacement curve. PP deforms in this SEN test brittle over the whole test speed range. The 30% blend is ductile over the whole studied test speed range.

At low speed ( $\leq 10^{-3}$  m/s) the start of crack propagation was determined by visual observation of the specimen during fracture. At high test speed ( $> 10^{-3}$  m/s) crack propagation was assumed to start at the maximum stress.

#### 3.2.1. Maximum stress

The stress displacement curves obtained by an SEN tensile test for the 30 vol% blend at varying test speed are shown in Fig. 5. The maximum stress of this 30% blend increases with test speed and considerable plastic deformation is taking place during crack propagation. Over the whole studied test speed range this 30% blend fractures ductile. If yielding in the notch is taking place the maximum stress is the yield stress or the fracture stress. If no yielding is taking place the maximum stress is the fracture stress of a brittle material. This maximum stress is the net cross-sectional stress, neglecting the stress concentration at the notch tip.

The maximum stress as function of test speed of polypropylene and the 30% blend are given in Fig. 6. For comparison also the yield stress measured for unnotched specimens are given. PP at low strain rate ( $10^{-3}$  s<sup>-1</sup>) has a maximum stress which almost equals the yield stress. This suggests that the notch is blunted and the whole cross-section ahead of the notch sustains a yield stress. At intermediate test speed the maximum stress of PP curve drops to well below the yield stress curve and crack propagation starts before the entire cross-section is bearing a yield stress. If the material fractures before yielding in the notch has

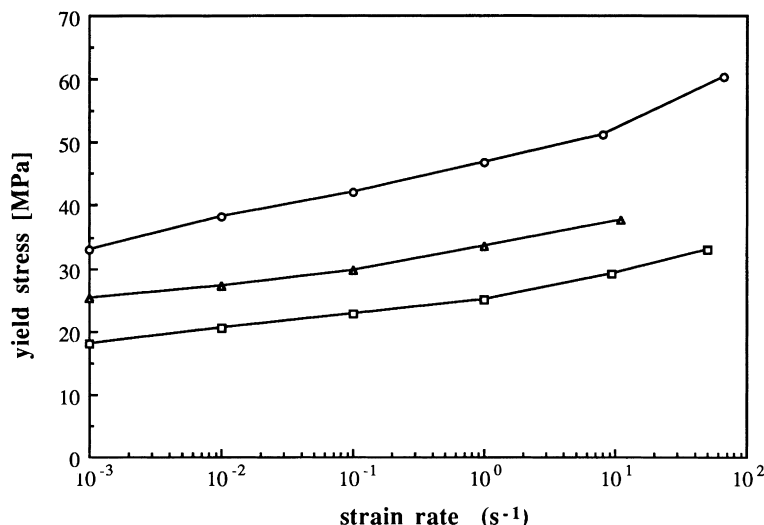


Fig. 3. Yield stress as a function of test speed for pure polypropylene and PP-EPDM blends. Rubber content [vol%]: ○: 0; △: 15; □: 30.

taken place, then a strong decrease in fracture stress is expected. This is not observed in PP at these strain rates at 20°C and even not at −40°C [16]. The 30% blends has nearly over the whole strain rate region a maximum stress which equals the yield stress. At very high strain rates a strong increase in stress is observed. A similar increase can be seen for the unnotched tensile results. This increase seems to be typical for materials with a strong plastic deformation in the notch.

### 3.2.2. Initiation

The initiation displacement (ID) (Fig. 7(a)) and initiation energy (IE) (Fig. 8(a)) are high at low test speeds and decrease with increasing test speed. At very high test speed the ID and IE appear to stabilise or even increase. The blends have, over the whole test speed range studied, a strong plastic deformation before the initiation of a crack.

### 3.2.3. Crack propagation

The crack propagation displacement (CPD) (Fig. 7(b))

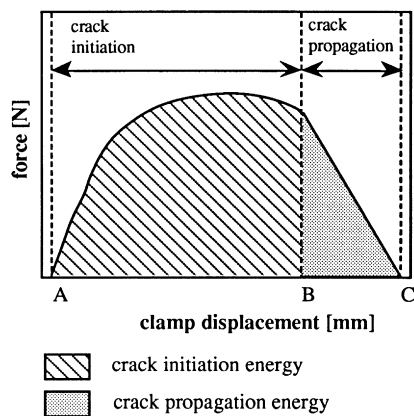


Fig. 4. Schematic force displacement graph as obtained by SEN measurements.

and the crack propagation energy (CPE) (Fig. 8(b)) curves are complex. At low test speeds the CPD decreases with increasing test speed as expected as with increasing test speed the fracture strain decreases. Surprisingly, at intermediate test speeds the CPD increases with increasing test speed. At very high test speeds they decrease again. The transition from brittle to ductile can be studied as function of test speed ( $V_{bd}$ ). With increasing rubber content the CPD increases and the test speed at which the blends become brittle (CPD equals zero) ( $V_{bd}$ ) increases. It should be noted that the brittle-ductile transition speed of the 5 vol% blend is considerably lower than that of the other blends.

CPE shows a comparable behaviour as the CPD with test speed. The anomalous behaviour however is stronger in the case of CPE. The crack propagation energy is approximately proportional to the product of maximum stress and CPD. The increase in the CPE is stronger than that of the CPD since the maximum stress also increases with test speed. The results suggest that at low test speed with increasing test speeds, the materials turn brittle. However at intermediate test speeds for all samples at  $10^{-2}$ – $10^{-1}$  m/s this trend is changed to a less brittle behaviour. At even higher test speeds the materials turn brittle again. The rubber content has a strong effect on where the blend starts to behave brittle. The higher the rubber content the higher the speed at which the blend become brittle. The turning ductile at  $10^{-2}$ – $10^{-1}$  m/s suggests that at this speed the deformation process undergoes a change. The change is probably as a result of an adiabatic plastic deformation. This suggest a strong warming up of the sample at high test speeds. A similar complex behaviour of the CPE with test speed was found for rubber modified nylon and this was there explained as a thermal blunting effect [4,7].

### 3.2.4. Total fracture process

The total fracture displacement (Fig. 7(c)) and fracture

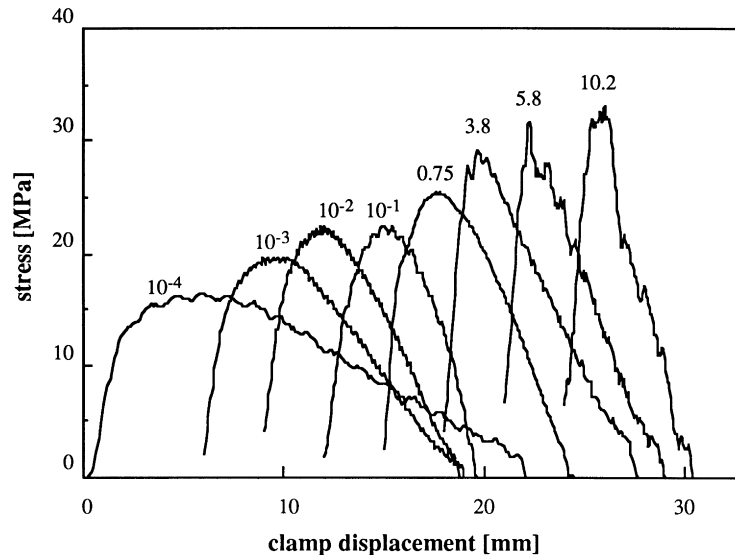


Fig. 5. Stress displacement curves obtained by an SEN tensile test for the 30 vol% PP-EPDM blend for different test speeds [m/s].

energy (Fig. 8(c)) show complex behaviour as function of test speed too. The fracture displacement and the fracture energy are about equally dependent on the initiation and the propagation part of the deformation. Over the whole test speed range the fracture displacements as well as the fracture energy increases with rubber concentration and this effect is strong.

### 3.2.5. Brittle–ductile transition

The brittle–ductile transition is defined as the onset of ductility. The energy supplied during crack propagation is a measure of the ductility. The crack propagation displacement is used as a measure of ductility. The brittle–ductile transition speed ( $V_{bd}$ ) is defined as the test speed at which the crack propagation displacement equals zero. For the PP and

the 1% blend the brittle–ductile transition must be at very low test speeds. At the 10 vol% blend at 1 mm/s exhibits a brittle–ductile transition at 20°C [1]. For the 30 vol% blend and the 40 vol% blend this point was determined by extrapolating the CPD curve to zero. The  $V_{bd}$  as a function of the rubber content is shown in Fig. 9. The  $V_{bd}$  increases with increasing rubber content, and seems to increase stepwise between 10 and 15 vol%.

### 3.3. SEM fractography

To study the asymmetric deformation process in fractured notched samples, SEM micrographs are taken of the fracture zone next to the fracture surface in the middle of the samples. The effect of test speed on the structure of the

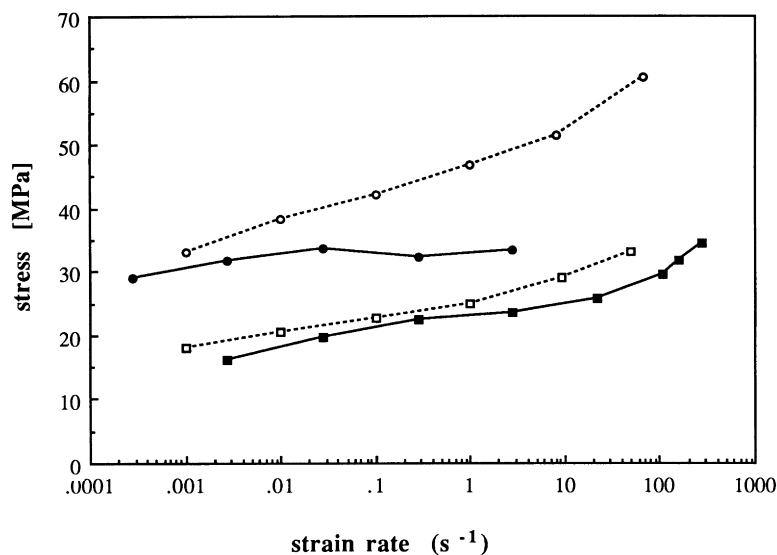


Fig. 6. Maximum stress during an SEN tensile test (full line) and the yield stress measured for unnotched specimen (dashed line) as a function of test speed for pure polypropylene and PP-EPDM blends. Rubber content [vol%]: ●: 0; ■: 30.

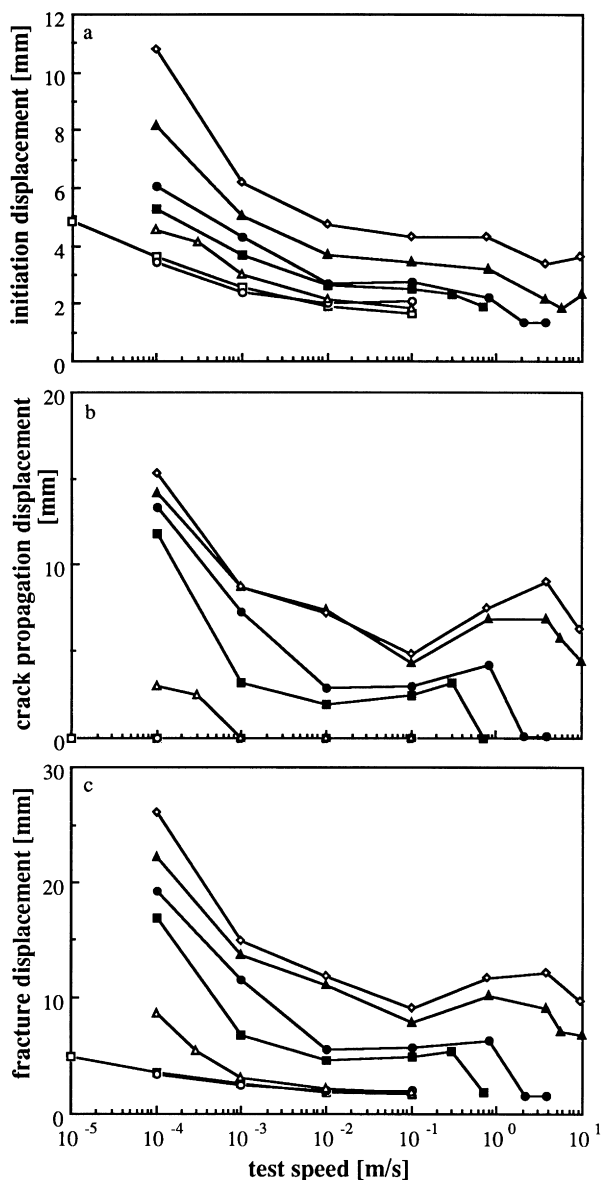


Fig. 7. Displacement during SEN tensile tests as a function of the test speed for pure polypropylene and PP-EPDM blends. Rubber content [vol%]: □: 0; ○: 1; △: 5; ■: 15; ●: 20; ▲: 30; ◇: 40.

fracture zone is studied on a 30 vol% blend of samples all of which fractured in a ductile manner (Fig. 10). Without deformation the rubber particles are spherical but they cannot be seen if they have not cavitated (or extracted by a solvent). The dark spots on the photos represent voids which are caused by cavitation of the rubber particles. If the voids are cigar-shaped they are elongated due to plastic deformation of the surrounding matrix. At low test speed, a clear deformation layer leading up to the fracture surface is observed with a strong elongation of the cavities. At higher test speed ( $\geq 0.1$  m/s) the deformation of the cavities seem to be less than at low speeds and a layer without cavities appears. The lower elongation of the cavities might be due to less deformation or to relaxation of the blend after

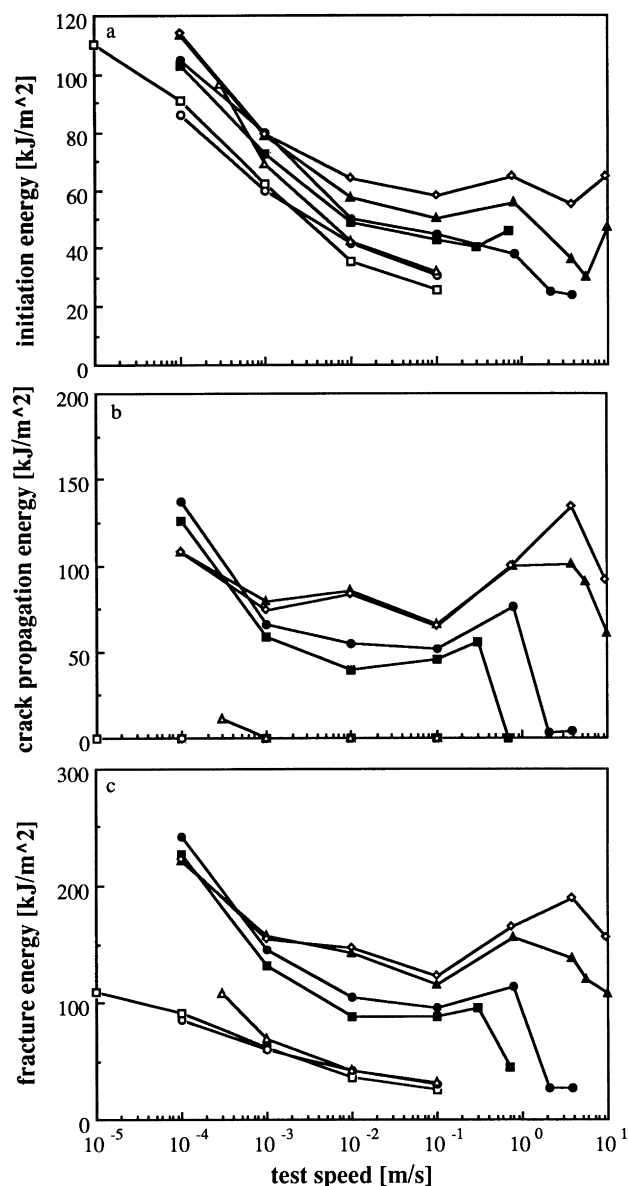


Fig. 8. Supplied energy during SEN tensile tests as a function of test speed for pure polypropylene and PP-EPDM blends. Rubber content [vol%]: □: 0; ○: 1; △: 5; ■: 15; ●: 20; ▲: 30; ◇: 40.

fracture. This might be due to the temperature increases at these high test speeds. At high temperatures the PP becomes elastic and after releasing the stress considerable relaxation can take place and as a result less elongated cavities in the micrographs. The layer without cavities suggests a complete relaxation of the matrix material. At 10 m/s, only a cavitation layer and a relaxation layer are observed, which suggests that the entire deformation layer has relaxed at this very high test speed (high temperature). Up until about  $10^{-2}$  m/s, the cigar-shaped voids reach up to the fracture surface. The thickness of the strongly deformed layer is about 100  $\mu\text{m}$ . At 0.1 m/s, just beneath the fracture surface the cigar-shaped voids have disappeared. At 1 m/s a layer just beneath the fracture surface a layer without deformation

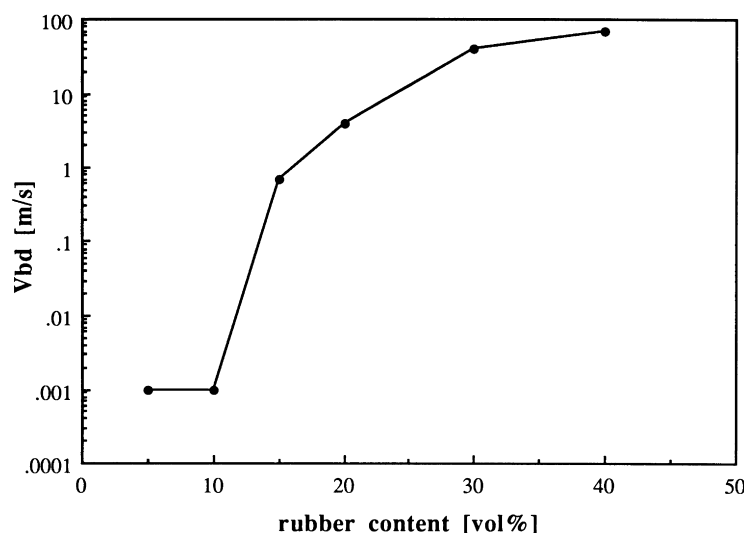


Fig. 9. The brittle–ductile transition speed ( $V_{bd}$ ) as a function of the rubber content for the PP–EPDM blends. The  $V_{bd}$  for the 10 vol% blend was obtained from van der Wal et al. [1]. The  $V_{bd}$  values of the 30 vol% blend and 40 vol% blend are obtained by extrapolating the CPD temperature curve to zero.

is present (thickness about 25  $\mu\text{m}$ ). At 10 m/s, all cigar-shaped voids have disappeared and a thick layer without cavities next to the fracture surface is present. The decrease in elongation of the voids at 0.1 and 1 m/s as the fracture plane is approached and the absence of voids next to the fracture surface in the 1 and 10 m/s samples suggest a disappearing of the voids. Voids can disappear if the highly oriented matrix layer surrounding the voids relaxes. Relaxation of oriented semi-crystalline polymers take place in the melt and if strong elastic recovery is possible. The appearance of the relaxation layer at high test speeds is also observed in nylon 6–EPR blends [4,5,7] and ABS [8]. In nylon 6–EPR blends and ABS, the thickness of the relaxation layer were respectively 3–5 and 0.5  $\mu\text{m}$ .

The appearance of the relaxation layer suggests that at the crack tip melting is taking place in PP–EPDM blends at the

high test speeds. The appearance of the relaxation layer coincides with the CPD increase with the test speed (Fig. 7).

### 3.4. Infrared thermography

With an infrared camera the temperature development of a sample in a SEN test was studied. The surface temperatures were recorded. The surface temperatures might well be different from the temperature in the sample. It is expected that at the surface, where there is a plain stress state the deformation zone thickness might well be larger than in the sample. The limitations of the used method is that the sampling rate is only 25 frames per second and that the resolution is not so high (140  $\mu\text{m}$ ) (Table 1).

An infrared thermograph obtained at initiation of the 5 vol% blend at  $10^{-3}$  m/s is shown in Fig. 11. At this low

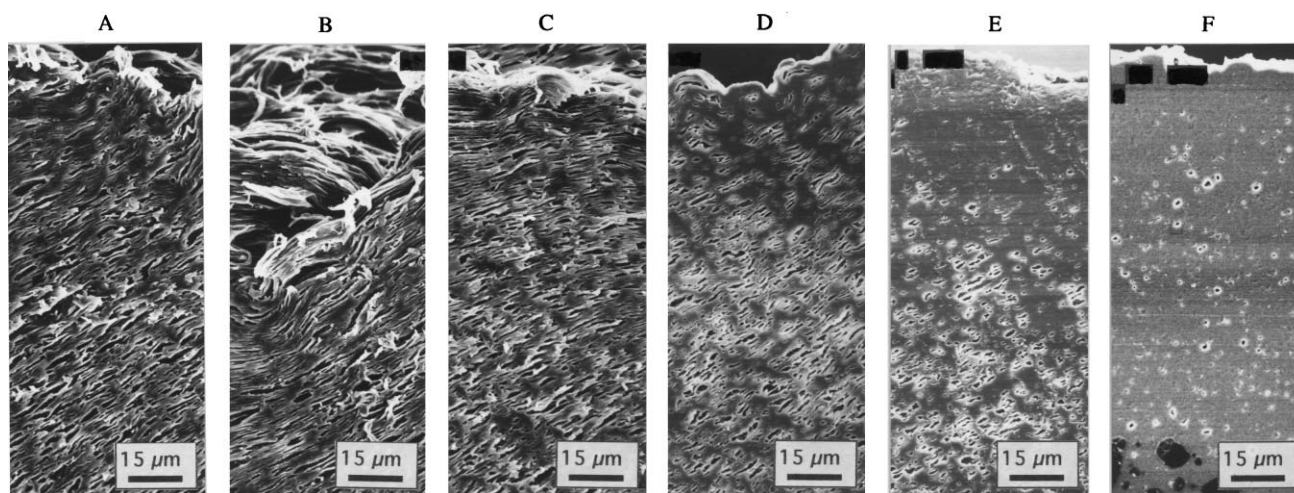


Fig. 10. SEM micrographs of the fracture zone at different test speeds for the 30 vol% PP–EPDM blend. Test speed [m/s]: A:  $10^{-4}$ , B:  $10^{-3}$ , C:  $10^{-2}$ , D:  $10^{-1}$ , E: 0.8, F: 10. The crack propagated from the left to the right, the fracture surface is located at the top.

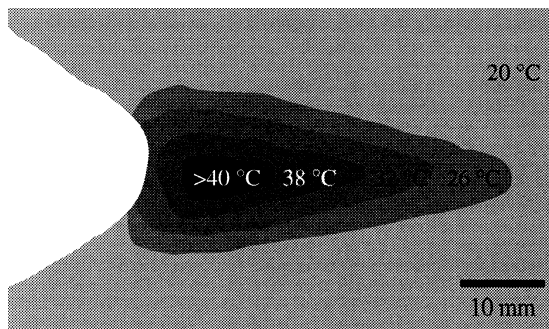


Fig. 11. Temperature development in notch zone at initiation of the 5 vol% blend at  $10^{-3}$  m/s.

test speed a clear temperature increase can be observed in front of the notch tip. The size and shape of the zone give information about the plastic deformation ahead of a notch. It can be assumed that the shape of the heating pattern equals the plastic deformation zone. The plastic deformation zone is therefore a line zone also called a Dugdale-like zone. The Dugdale-like zone is a result of inhomogeneous plastic deformation, with strain softening. Fig. 12 shows the height to length ratio of the plastic zone as a function of the rubber content at various test speeds. With increasing rubber content, and to a lesser extent, with increasing test speed, the height to length ratio increases. In other words, the line plastic zone turns into a circular plastic zone. This suggests with increasing rubber content a change from inhomogeneous deformation to a more homogeneous deformation.

The maximum temperature is ahead of the notch. The influence of test speed on this maximum surface temperature during crack initiation is shown in Fig. 13. Based on extrapolation of the temperature rise versus test speed curve the temperature rise starts at test speeds as low as  $10^{-5}$  m/s. The temperature increases almost linearly with the logarithm of test speed and decreases with increasing rubber content. This decrease in temperature with rubber content

can possibly be explained by the much larger initiation deformation (ID) (Fig. 7(a)) and thus the lower strain rate if one takes into account that part of the ID is elastic deformation.

An infrared thermograph of a running crack at  $10^{-3}$  m/s for the 30 vol% blend is shown in Fig. 14. There is a large heating zone in front of the crack tip. The size of the heating zone in the direction perpendicular to the fracture surface was determined at the point where the crack penetrates half the width of the sample. A  $28^{\circ}\text{C}$  isotherm was used as a boundary for the heating zone in order to diminish disturbances by heat diffusion. The size of the heating zone as a function of the test speed at varying rubber content is shown in Fig. 15. With increasing test speed the size of the heating zone decreases. As the yield stress increases with strain rate it can be expected that the yield strain decreases. At very high test speeds the width of the deformation zone increases again. We observed a similar behaviour in the crack propagation displacement (CPD) (Fig. 7(b)).

The temperature rise in the blends during crack propagation versus the test speed is shown in Fig. 16. Regardless of the plateau at intermediate test speed, the temperature rise increases almost linearly with the logarithm of the test speed and ranges from  $30^{\circ}\text{C}$  at  $10^{-4}$  to around  $90^{\circ}\text{C}$  at 10 m/s. Based on extrapolation of the temperature rise versus test speed curve the temperature increase begins at about  $10^{-5}$  m/s. At test speeds in excess of  $10^{-5}$  m/s, the plastic deformation process in front of the crack tip turns from isothermal to adiabatic. The observed linear temperature increase up to the very high test speeds suggest that fully adiabatic deformation is not easily taking place. A reason for this might be the asymmetric nature of plastic deformation layer with only a very thin layer which is highly deformed. The strongly deformed layer is only  $100\text{ }\mu\text{m}$  thick and the relaxation layer  $25\text{ }\mu\text{m}$ . The temperature development can be approximated [5]. Also the speed at which a running crack behaves adiabatic can be calculated

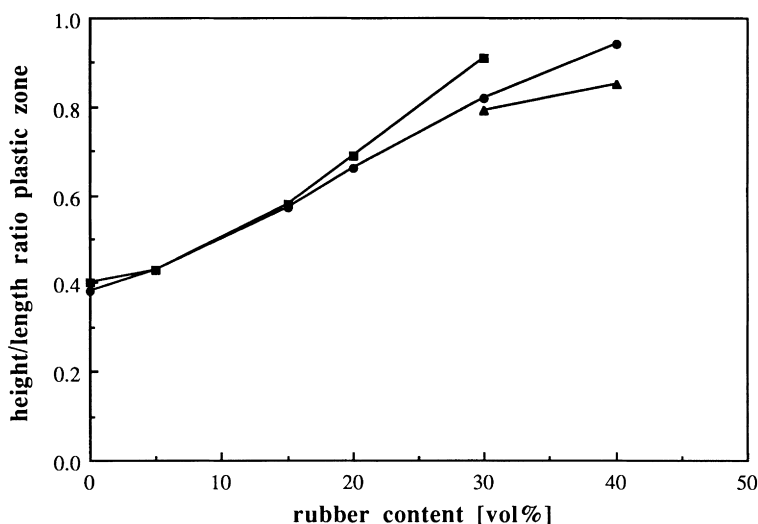


Fig. 12. The height/length ratio of the heating zone versus the rubber content at various test speeds. Test speed [m/s]:  $\square$ :  $10^{-4}$ ;  $\circ$ :  $10^{-3}$ ;  $\triangle$ :  $10^{-2}$  m/s.

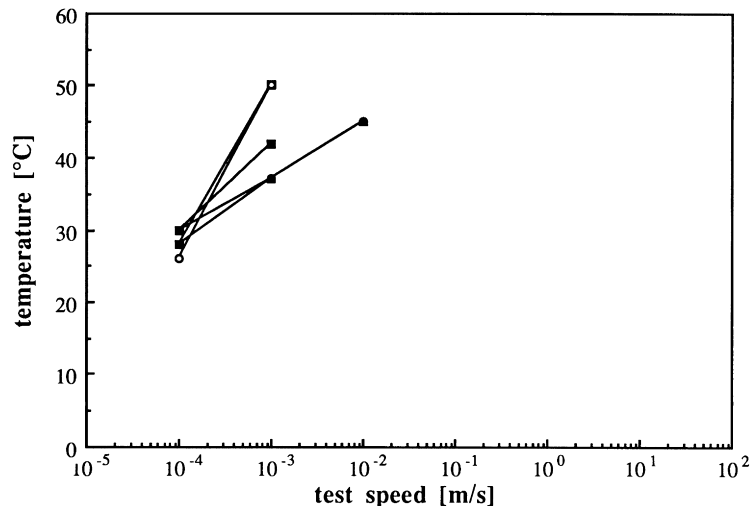


Fig. 13. Temperature development during initiation as a function of the test speed for polypropylene and PP-EPDM blends, at room temperature. Rubber content [vol%]: □: 0; ○: 5; ■: 15; ●: 30; ▲: 40.

[3,5]. With a 100  $\mu\text{m}$  deformation layer the calculated speed at which adiabatic deformation is taking place is at speeds higher than  $10^{-1}$  m/s.

The observed maximum surface temperatures at 1 m/s are high (90°C) but much lower than the melting temperature (170°C). The recorded sample surface temperature are, for a number of reasons, not representative for 25  $\mu\text{m}$  relaxation layer in the sample. The resolution of the camera is only 130  $\mu\text{m}$  not enough to see the 25  $\mu\text{m}$  melt layer or the 100  $\mu\text{m}$  strongly deformed layer. The deformation zone thickness might on the surface well be larger than in the sample as a result of a lower strain. The important finding is that at high test speeds considerable temperature increase is taking place and that isothermal deformation of PP blends for test speeds higher than  $10^{-5}$  m/s cannot be assumed.

#### 4. Conclusions

The notch deformation of PP-EPDM blends as function of test speed is complex. At low test speed the crack propagation displacement (CPD) and the crack propagation energy (CPE) decrease rapidly with increasing test speed. However, at intermediate test speed ( $>10^{-2}$  m/s) the CPD and CPE increase with increasing test speed. This abrupt increase in CPD and CPE cannot be explained by the gradual increase in temperature. However at this speed the structure of the deformation zone (of the 30% blend) next to the fracture surface changes. At this speed the samples are supposed have a layer which must have been relaxed. This suggests that during the plastic deformation at high test speeds, at head of the notch, a relaxation layer is formed and this layer may blunt the notch—a thermal blunting

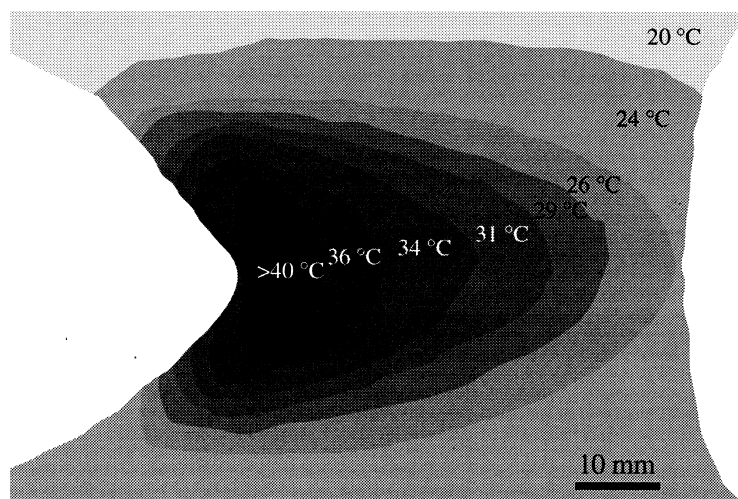


Fig. 14. Infrared thermograph of a running crack at  $10^{-3}$  m/s for the 30 vol% blend.

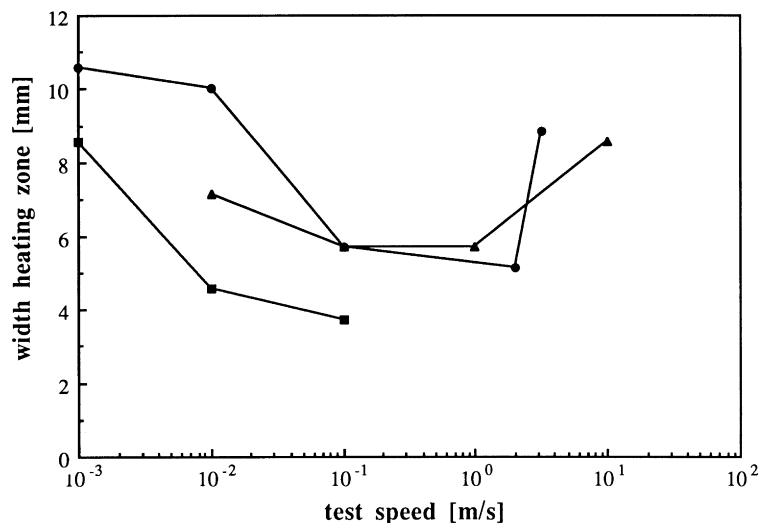


Fig. 15. The heating zone width in the middle of the sample as a function of test speed at varying rubber content. Rubber content [vol%]: ■: 15; ●: 30; ▲: 40.

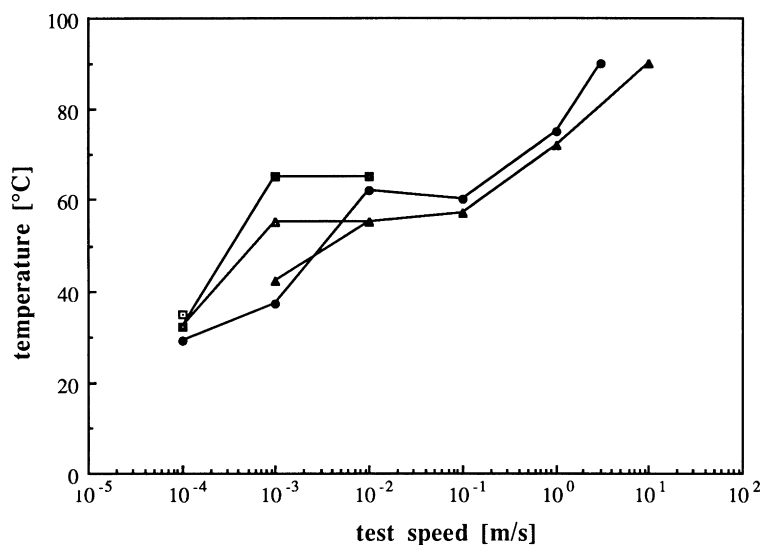


Fig. 16. Temperature development during crack propagation as a function of the test speed for PP-EPDM blends. Rubber content [vol%]: ○: 5; △: 10; ■: 15; ●: 30; ▲: 40 vol%.

process. The observed two processes might be fracture process at low test speeds with strong plastic deformation both during initiation and during propagation process and at high speeds plastic deformation process with the formation of an elastic layer ahead of a notch. This thermal blunting process considerably enhances the toughness and without this process these blends might well be brittle at high test speeds.

### Acknowledgements

We would like to thank Prof Dr Ir L.C.E. Struik for helpful discussions and comments. This work is part of the research programme of the Twente University.

### References

- [1] van der Wal A, Nijhof R, Gaymans RJ. *Polymer* 1999;40:6031.
- [2] van der Wal A, Verheul AJJ, Gaymans RJ. *Polymer* 1999;40:6057.
- [3] Godovsky YK. *Thermophysical properties of polymers*. New York: Springer, 1992 Chap 8, pp 149.
- [4] Dijkstra K, ter Laak J, Gaymans RJ. *Polymer* 1994;35:315.
- [5] Dijkstra K, Gaymans RJ. *J Mater Sci* 1994;29:3231.
- [6] Dijkstra K, Wevers HH, Gaymans RJ. *Polymer* 1994;35:315.
- [7] Janik H, Gaymans RJ, Dijkstra K. *Polymer* 1995;36:4203.
- [8] Janik H, Streenbrink SA, Gaymans RJ. *J Mat Sci* 1997;32:5505.
- [9] Béguelin Ph, Kausch HH. In: Williams JG, Pavan A, editors. *Impact and dynamic fracture of polymers and composites*, London: Publ. Mechanical Engineering Publications Ltd, 1995. pp. 1 ESIS no 19.
- [10] Williams JG, Braga L, MacGillivray HJ. In: Williams JG, Pavan A, editors. *Impact and dynamic fracture of polymers and composites*, London: Publ. Mechanical Engineering Publications Ltd, 1995 ESIS no 19, pp. 45.

- [11] Leevers PS, Morgan RE. *Engng Fracture Mech* 1995;52:999.
- [12] Leevers PS, Douglas M, Chong M, Williams JG. *Deformation, yield and fracture of polymers*. London: Institute of Materials, 1997 pp. 106.
- [13] Williams JG. *Fracture mechanics of polymers*. Chichester, England: Ellis Horwood, 1984 Ch. 8.
- [14] Williams JG, Adams GC. *Int J Fracture* 1987;33:209.
- [15] Accessory Lenses and Filters, IQ 812, Flir Systems, A-11/93 IQ 812, Flir systems.
- [16] van der Wal A, Mulder JJ, Thijs HA, Gaymans RJ. *Polymer* 1998;39:5967.